IJAME

Int. J. of Applied Mechanics and Engineering, 2023, vol.28, No.3, pp.101-111
DOI: 10.59441/ijame/172900

STAGNATION-POINT FLOW OF WILLIAMSON FLUID ALONG A STRETCHED PLATE WITH CONVECTIVE THERMAL CONDITION AND ACTIVATION ENERGY

S.O. SALAWU
Department of Mathematics, Bowen University, Iwo, NIGERIA
E-mail: kunlesalawu2@gmail.com

The implication of a stagnation-point flow together with the influence of activation energy in a Williamson fluid, which consists of tiny particles, over an expansive plate is analyzed numerically. Conditions of convective heat and mass motion with features of irregular movement and thermal-migration of particles influenced by viscous dissipation and convective heat surface condition are checked in the study. The conversion of the model equations from the initially formulated partial derivatives to ordinary ones is implemented by similarity transformations while an unconditionally stable Runge-Kutta-Fehlberg integration plus shooting technique are then used to complete the integration. Various interesting effects of the physical parameters are demonstrated graphically and explained appropriately in order to make accurate predictions. Moreover, the accuracy of the solution is verified by comparing the values of the skin friction factor with earlier reported ones in literature under limiting constraints. It is worth mentioning that the velocity profiles flatten down as the magnitude of the magnetic field factors expands but this causes a boost in the fluid's temperature. The concentration field also appreciates with activation energy but depreciates with chemical reaction and Schmidt number.

Key words: activation energy; Williamson fluid; stagnation-point; convective condition.

1. Introduction

Many industries, including those that produce polymers, have found it useful to study the boundary layer flow originated by expanding materials, including wire drawing, glass and polymer processes, textile and paper production, etc. [1]. Crane [2] discussed a the solution to such problem in a closed-form precise manner for a time-independent motion induced by an extending plate. After such brilliant introduction a vast number of scholars [3-5] have engaged the phenomenon taking into account the relevant factors of interest [6-8]. Besides, various categories of fluids have been studied on stretchable devices by scientists and researchers. However, much time and energy have been given to analyze non-Newtonian fluids because of the vast range of fields in which such knowledge may be useful. For instance, in the fields of oil drilling, fluid suspensions, molten polymers, mud drilling, medicines, plus other engineering activities. A great number non-Newtonian fluids models exist due to inability of any constitutive model to account for the whole range of fluid properties, examples are: the Williamson, micropolar Casson, Maxwell fluid and many more [9-10].

The Williamson fluid has its inherent shear thinning trait, in which an increase in the shear stress rate results in a drop in viscosity. The fluid dynamics of plasma, blood, and emulsion sheets like photographic films fall under this umbrella of Williamson fluid [11]. Many scholars have evaluated various physical terms on this particular fluid with reports on various configurations of geometry, parameters, and boundary conditions. When investigating the effects of the Williamson fluid on Blasius flow, stretching flow, and stagnation, Khan and Khan [12] used a homotopy analytic approach. Additionally, Hayat *et al.* [13] analyzed the unsteady flow of such fluids via a permeable stretchable sheet linked with thermal radiation and Ohmic heating, while Megahed [14] enhanced such research by using a nonlinear stretched sheet related with dissipative effects.

Stagnation point flow research has practical applications in emergency shut down cooling of nuclear reactors, fan-based cooling of electronic goods, aerodynamic extrusion of plastic sheets, and many other areas [15-16]. When a fluid invades a solid, the fluid velocity at the site of intrusion is zero, and the pressure, heat transfer, and mass deposition are all at their peak. Scientists have now found better solutions to this kind of phenomenon by taking into account flows on a variety of geometries while making a wide range of assumptions and constraints. For example, Chiam [17] studied this topic for a linearly stretching plate where the stretching velocity is proportional to the straining velocity, and Mohapatra and Gupta [18] expanded this work by including a uniform magnetic field under the influence of a prescribed surface heat flux and assuming varying velocities. The case of a nonlinear stretched surface corresponding to the Williamson fluid transport associated with the impact of radiation was discussed by Monica *et al*. [19], while Agbaje *et al*. [20] investigated the phenomenon with features of heat transfer characteristics being configured in a porous medium.

The term "nanofluid" refers to fluids that are made up of minute particles (nanoparticles) of metals, oxides, etc. [21]. When compared to traditional base fluids, the thermal conductivity of this new kind of fluid is much higher. It is essential to improve the cooling process in high-energy equipment because many technological, engineering and manufacturing processes, such as power manufacture and atomic reactors, need the heating and cooling of fluids. The wide range of potential applications of nanofluids research, including the pharmaceutical and industrial cooling sectors, the transportation sector, and the cooling of electronic component. A lot of researchers have deliberated on this concept as found in [22-26].

In engineering and industrial projects, thermal radiation is a must (e.g. hot rolling, solar power technology, gas turbines, etc.). The understanding of this concept is necessary for developing energy conversion appliances when a high-temperature differential is present in the flow field. Because of the importance of such a concept to a wide range of engineering operations as listed above, researchers have discussed it in various manner. For instance, Mukhopadhyay *et al*. [27] evaluated such a phenomenon on a Newtonian fluid and Ullah *et al*. [28] performed a numerical analysis on the topic with a nonlinear stretching sheet and Newtonian heating condition. Fatunmbi *et al*. [29] recently examined such a phenomenon on the micropolar fluid using the spectral quasi-linearization approach, while Patel [30] analytically treated such an issue using the Casson fluid and taking cognizance of nonlinear radiation.

The emphasis in this investigation is to simulate the implication of stagnation-point flow with activation energy on the Williamson fluid consisting of tiny particles over an expansive plate with convective heat condition at the surface. The important practical applications in engineering and industries have motivated this study. The model also takes into account the consequence of thermal radiation, viscous dissipation in the field of energy plus chemical reaction and Brownian movement in the concentration region. The essential contributions of the involved parameters are demonstrated via a variety of graphs with proper explanation for reasonable prediction for the end users.

2. Formulating the problem

Formulation of the problem at hand requires stating the assumptions for modelling and then writing the expressions for the governing equations. The flow under investigation is a two-dimensional, incompressible and steady hydromagnetic Williamson nanofluid passing an expansive plate characterized by coordinate (x,y) with (u,v) as the respective components of velocity. An equal but opposing force is applied at the extending plate in a way to make the origin stable when $y=0$. Thus, it is supposed that the motion is occasioned by the extending plate with features of tiny particles. It is believed that the perpendicular axis to the movement is y whereas the movement of the fluid is along x. There is an imposition of a magnetic field from the external region in a way normal to the direction of the x axis (see Fig.1) but the internal magnetic field impact is ignored in the analysis. All fluid characteristics are believed to be constant, the heat condition at the surface is convective in nature as shown in Eq.(2.5). More so, the concentration region comprises of chemical reaction, activation energy plus Brownian movement and thermophoresis forces.

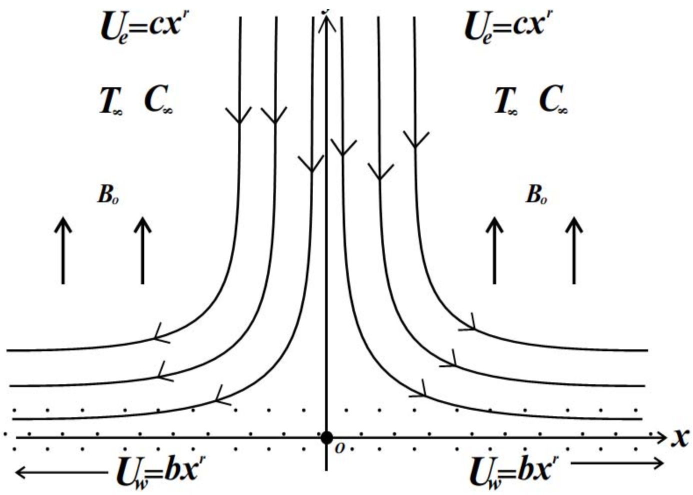

Fig.1. The flow geometry.

The combination of these assumptions as highlighted above in conjunction with the famous boundary layer approximation rule leads to, Eqs (2.1)-(2.4) which are the equations which properly define the current problem under study.

$$\frac{\partial u}{\partial x}+\frac{\partial v}{\partial y}=0, \tag{2.1}$$

$$u\frac{\partial u}{\partial x}+v\frac{\partial u}{\partial y}=u_\infty\frac{du_\infty}{dx}+\frac{\mu}{\rho}\frac{\partial^2 u}{\partial y^2}+\sqrt{2}\Gamma\left(\frac{\partial u}{\partial y}\right)\frac{\partial^2 u}{\partial y^2}-\frac{\sigma}{\rho}B_0^2\left(u-u_\infty\right), \tag{2.2}$$

$$\begin{gathered}u\frac{\partial T}{\partial x}+v\frac{\partial T}{\partial y}=\frac{K}{\left(\rho c_p\right)}\left(1+\frac{16\sigma^\star T_\infty^3}{3k_1K}\right)\frac{\partial^2 T}{\partial y^2}+\Upsilon\left[\frac{D_w}{T_\infty}\left(\frac{\partial T}{\partial y}\right)^2+Ds\left(\frac{\partial T}{\partial y}\frac{\partial N}{\partial y}\right)\right]+ \\ +\frac{\sigma B_0^2}{\left(\rho c_p\right)}(u-u_\infty)^2+\frac{\mu}{\left(\rho c_p\right)}\left(\left(\frac{\partial u}{\partial y}\right)^2+\Gamma\left(\frac{\partial u}{\partial y}\right)^3\right),\end{gathered} \tag{2.3}$$

$$u\frac{\partial N}{\partial x}+v\frac{\partial N}{\partial y}=Ds\frac{\partial^2 N}{\partial y^2}+\frac{D_w}{T_\infty}\left(\frac{\partial^2 T}{\partial y^2}\right)-Cr\left(N-N_\infty\right)\left(\frac{T}{T_\infty}\right)^a\exp\left(-\frac{E_e}{\lambda T}\right). \tag{2.4}$$

At the boundary, the following conditions hold valid:

$$\begin{gathered}u=u_w=mx,\quad v=0,\quad -K\frac{\partial T}{\partial y}=B_t\left(T_f-T_\infty\right),\quad N=N_s\ \text{ at }\ y=0, \\ u\to u_\infty=cx,\quad T\to T_\infty,\quad N\to N_\infty\ \text{ as }\ y\to\infty.\end{gathered} \tag{2.5}$$

We have introduced the stream functions $u=\frac{\partial\psi}{\partial y}, v=-\frac{\partial\psi}{\partial x}$ and the similarity variables associated with non-dimensional quantities in Eq.(2.6) to restructure the partial derivatives governing the problem to ordinary differential variables.

$$\eta=\sqrt{\frac{mx}{\vartheta}}y,\quad \psi=\sqrt{\vartheta mx}f(\eta),\quad \theta(\eta)=\frac{T-T_\infty}{T_f-T_\infty},\quad \phi(\eta)=\frac{N-N_\infty}{N_s-N_\infty},\quad We=\Gamma\sqrt{2\frac{m^3x^{3r-1}}{\vartheta}},$$

$$\delta=\frac{\left(T_f-T_\infty\right)}{T_\infty},\quad Pr=\frac{\mu c_p}{K},\quad M=\frac{\sigma B_0^2}{m\rho},\quad Nr=\frac{16\sigma^\star T_\infty^3}{3k^\star K},\quad Ec=\frac{U_w^2}{C_p\left(T_s-T_\infty\right)},$$

$$Sc=\frac{\nu_\infty}{Ds},\quad \gamma_1=\frac{Cr}{m},\quad AE=\frac{Eb}{bT_\infty},\quad h=\frac{B_t}{K}\sqrt{\frac{\vartheta}{m}},\quad Nb=\frac{(\rho c_p)_p D_s\left(C_w-C_\infty\right)}{(\rho c_p)_f\vartheta}, \tag{2.6}$$

$$NT=\frac{\left(\rho c_p\right)_p D_s\left(Tf-T_\infty\right)}{\left(\rho c_p\right)_f T_\infty\vartheta},\quad \Upsilon=\frac{(\rho c)_p}{(\rho c)_f},\quad A=\frac{c}{m}.$$

Consequent upon using Eq.(2.6) there is assurance of validity of the continuity Eq.(2.1) whereas Eqs (2.2)-(2.4) together with wall constraints (2.5) are changed to the under listed ordinary derivatives.

$$\left(1+We\frac{\partial^2 f}{\partial\eta^2}\right)\frac{\partial^3 f}{\partial\eta^3}+f(\eta)\frac{\partial^2 f}{\partial\eta^2}-\left(\frac{\partial f}{\partial\eta}\right)^2+A^2-M\left(\frac{\partial f}{\partial\eta}-A\right), \tag{2.7}$$

$$\begin{gathered}(1+Nr)\frac{\partial^2\theta}{\partial\eta^2}+Pr\left(f\frac{\partial\theta}{\partial\eta}+NT\left(\frac{\partial\theta}{\partial\eta}\right)^2+NB\frac{\partial\theta}{\partial\eta}\frac{\partial\phi}{\partial\eta}\right)+\\ +PrEc\left(1+\frac{We}{\sqrt{2}}\frac{\partial^2 f}{\partial\eta^2}\right)\left(\frac{\partial^2 f}{\partial\eta^2}\right)^2+PrEcM\left(\frac{\partial f}{\partial\eta}-A\right)^2,\end{gathered} \tag{2.8}$$

$$\frac{\partial^2\phi}{\partial\eta^2}+\frac{NT}{NB}\frac{\partial^2\theta}{\partial\eta^2}+Scf(\eta)\frac{\partial\phi}{\partial\eta}-Sc\xi\left(1+\delta\theta(\eta)\right)^a\exp\left(-\frac{AE}{1+\delta\theta(\eta)}\right)\phi(\eta). \tag{2.9}$$

The main equations depend on the following wall constraints for validity

$$\begin{gathered}\frac{\partial f}{\partial\eta}-1=0,\quad f(\eta)=0,\quad \frac{\partial\theta}{\partial\eta}=-h\left(1-\theta(\eta)\right),\quad \frac{\partial\phi}{\partial\eta}-1=0\quad \text{at}\quad \eta=0,\\ \frac{\partial f}{\partial\eta}=A,\quad \theta(\eta)=0,\quad \phi(\eta)=0\quad \text{as}\quad \eta\to\infty.\end{gathered} \tag{2.10}$$

The physical quantities useful for the engineers are the skin frictional factor S_x, Nusselt H_x and the Sherwood Sh_x numbers which are respectively indicated in a dimensionless manner as follows:

$$S_x = \left(\frac{\partial^2 f}{\partial \eta^2} + \frac{We}{2}\left(\frac{\partial^2 f}{\partial \eta^2} \right)^2 \right), \quad H_x Re_x^{-0.5} = -(1+Nr)\frac{\partial \theta}{\partial \eta}, \quad Sh_x Re_x^{-0.5} = -\frac{\partial \phi}{\partial \eta} \quad \text{at} \quad \eta = 0. \quad (2.11)$$

3 Numerical procedures for the solution

Estimating the exact solution to the problem at hand is tedious because it involves nonlinear equations of higher order. Thus, we have implemented the solution through a numerical technique which is well-known as unconditionally stable Runge-Kutta-Fehlberg technique coupled with the method of shooting technique. Implementing this method means that a fixed value of η has to be picked and the system of ordinary derivatives (2.7)-(2.9) with the wall conditions (2.10) is transmuted into simultaneous equations of first order. This idea reduces the system of the BVP to IVP using the shooting method. After this, the initial conditions are obtained and the resultant equations are then solved simultaneously by means of Maple 2016. We have verified the precision of the solution obtained in this work with those earlier published in the literature as collated in Tab.1. There is a strong correlation in the values of S_x as gotten in this study with that of Mabood and Das [31], and Xu and Lee [32]).
The graphs have been plotted with the following values except if stated otherwise in the plots:

$$Ec = 0.2, \quad Nr = 0.1, \quad We = 0.3, \quad Sc = 0.62, \quad E = 0.1, \quad n = 0.2, \quad NT = 0.3,$$

$$NB = 0.5 = M, \quad Pr = 0.72, \quad A = 0.2, \quad \delta = \varsigma = 0.3, \quad h = 0.3.$$

Table 1. Summary of S_x values as related to published items for a variety of M values.

M	[31]	[32]	Current work
0	1.000008	-	1.0000
1.0	1.4142135	1.41421	1.4142
5.0	2.4494987	2.4494	2.4500
10.0	3.3166247	3.3166	3.3256
50.0	7.1414284	7.1414	7.1413
100.0	10.049875	10.0498	10.0456

4. Presentation and discussion of results

To see clearly the significant contributions of the physical quantities on the field of flow, a variety of graphs have been included in this section with necessary explanation for accurate prediction.

In Fig.2, there is a plot of the velocity field responding to variations in the magnetic field term M (0, 1, 2) when the stretching ratio term A is in place. It is clear that uplifting M acts inversely to the fluid motion. This is well-noted due to creation of the retarding Lorentz force to the electroconducting Williamson fluid by the magnetic field which in a transverse direction to the fluid. Therefore, when the strength of M increases, then a proportionate rise in the Lorentz force occurs such that there is a higher resistance to the movement of the fluid. However, the velocity profile behaves otherwise with higher values of A; an acceleration of fluid occurs by growing values of A. Then it can be concluded that the velocity profiles can be adjusted up by increasing the values of the velocity ratio term.

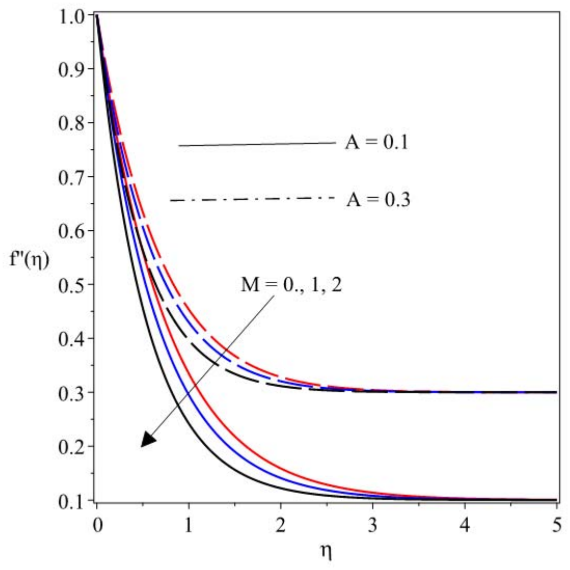

Fig.2. Velocity $f'(\eta)$ against the magnetic field term M .

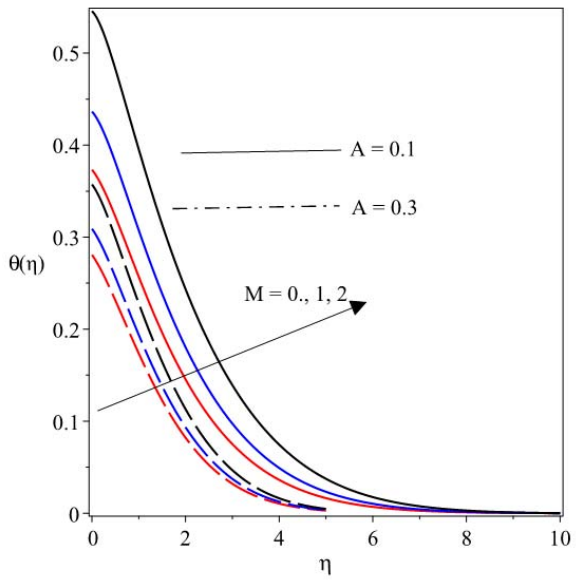

Fig.3. $\theta(\eta)$ against the magnetic field term M .

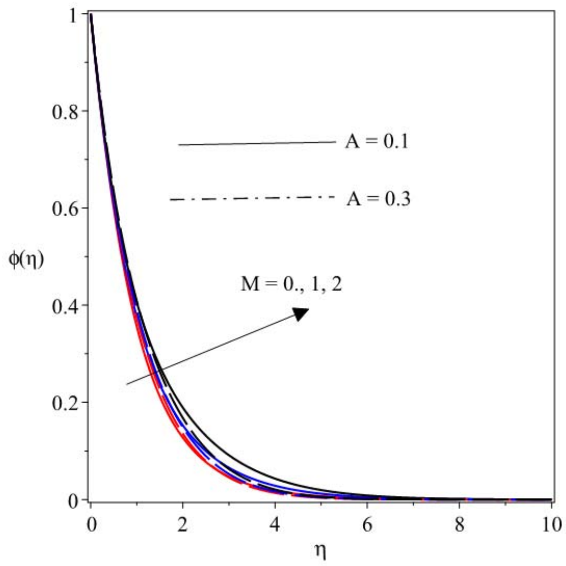

Fig.4. $\phi(\eta)$ against the magnetic field.

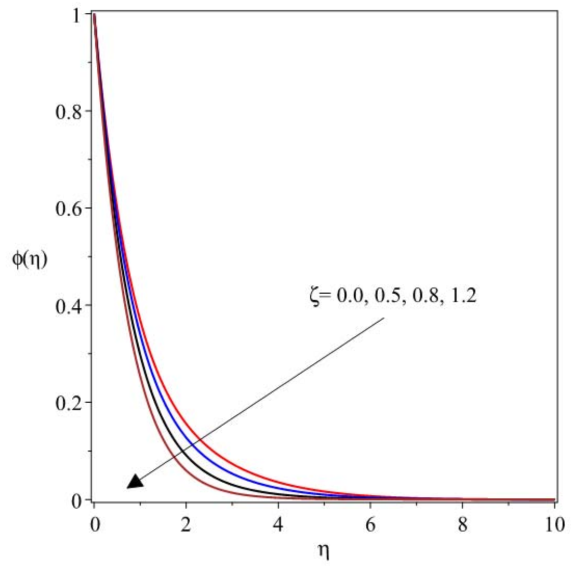

Fig.5. $\phi(\eta)$ against the chemical reaction term ζ.

A depleted concentration profile occurs when the intensity of the chemical reaction term ζ is raised as described in Fig.5. The chemical reaction parameter depreciates the concentration region as found in Fig.5. Whereas a higher value of thermophoresis term NT raises the thickness of the thermal boundary structure as well boosts the heat dissipation profile as displayed in Fig.6. In line with that, the surface convection term also called Biot number elevates the thermal region as it increases from *0.1* to *0.5* as indicated in Fig.6. The temperature and concentration fields act contrarily to that of the velocity profile when the values of M increase. With a growth in M , there is a higher temperature as indicated in Fig.3, while a rise in concentration profile is found in Fig.4 due to escalating values of M . Meanwhile the presence of A causes both temperature and concentration to fall as noticed in Figs 3 and 4.

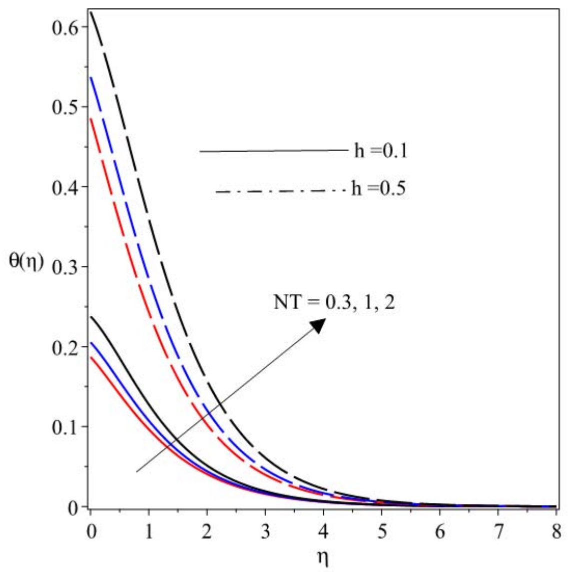

Fig.6. $\theta(\eta)$ versus thermophoresis term NT .

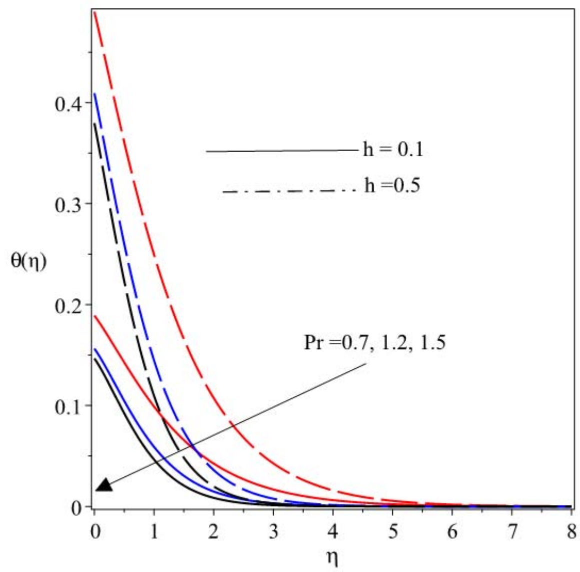

Fig.7. $\theta(\eta)$ versus Prandtl number Pr .

Raising the magnitude of the Prandtl number Pr (*0.7*, *1.2*, *1.5*) as found in Fig.7 causes a decline in the thickness of the thermal boundary and also compels a fall in the surface heat distribution. Irrespective of the value of the Biot number, heat distribution appreciates with NT while it decays with Pr as respectively demonstrated in Figs 6 and 7.

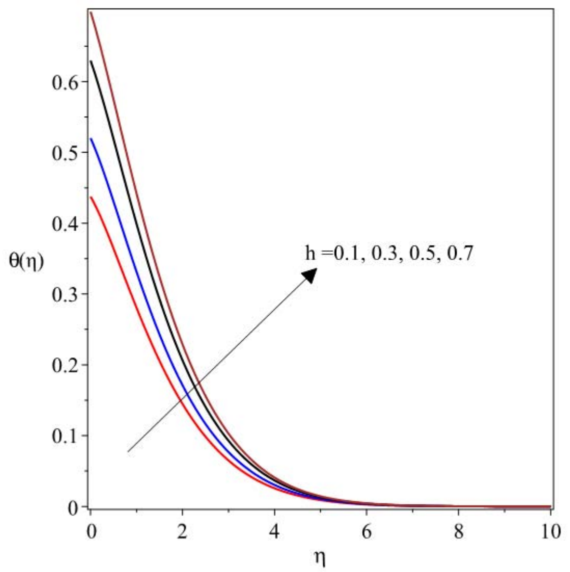

Fig.8. $\theta(\eta)$ versus the Biot number h .

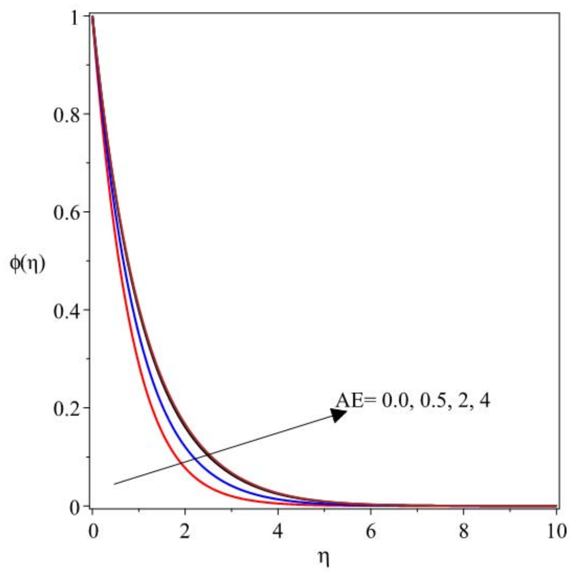

Fig.9. $\theta(\eta)$ versus the activation energy AE .

It is clearly shown in Fig.8 that a growth in $\theta(\eta)$ is directly proportional to a rise h. It can be said physically that the ratio of the internal and the boundary film heat resistance of the hot fluid under the surface defines h, i.e. the Biot number. In this view, a higher magnitude of h strengthens the apparent convection and thereby the encourages heat region to grow. In Fig.9, the impact of activation energy AE is revealed on the concentration region. Escalating nature of AE causes the thickness of the concentration wall layer to rise, thereby the concentration profiles enhance with *hke* in AE as indicated in this figure.

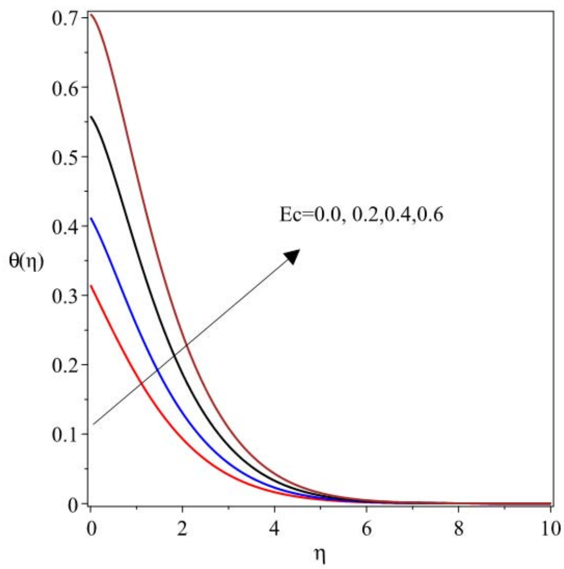

Fig.10. $\theta(\eta)$ versus the thermophoresis term NT.

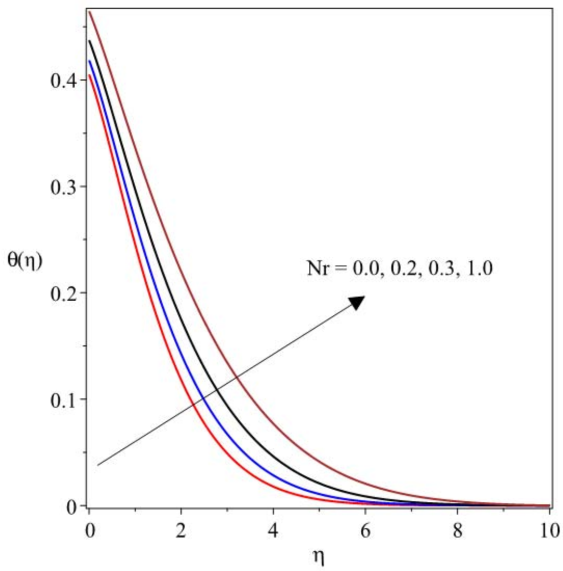

Fig.11. $\theta(\eta)$ versus the Prandtl number Pr.

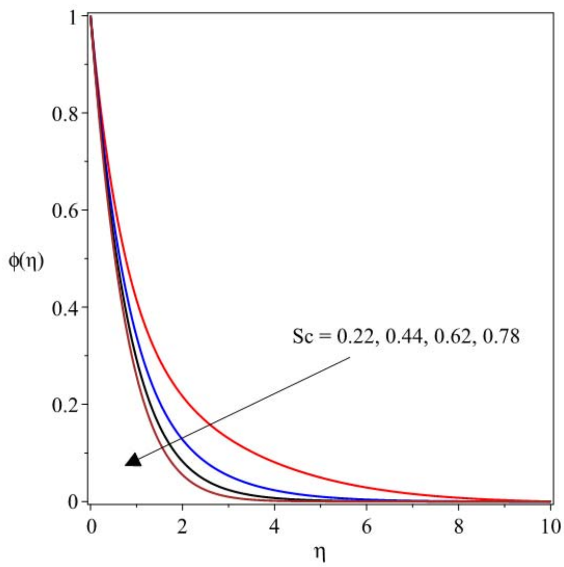

Fig.12. $\phi(\eta)$ versus the Schmidt number Sc.

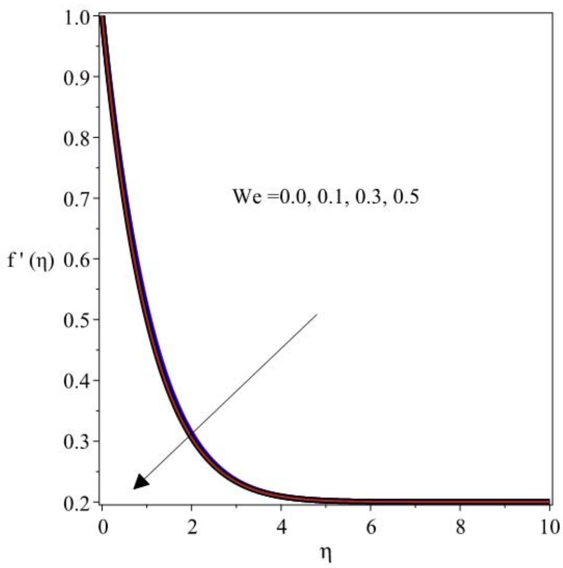

Fig.13. $f'(\eta)$ versus the Weissenberg number We.

The Eckert number encourages higher temperature profile as seen in Fig.10. Thus as Ec (*0.0*, *0.2*, *0.4*, *0.6*) moves up there is a hike in $\theta(\eta)$. This is as a result of frictional drag between the Williamson fluid particles and the extending plate. In line with that, Fig.11 depicts what happens in the heat profile when the thermal radiation term is raised. The heat boundary film becomes thicker with rising values of Ec and with that trend, there is an increase in $\theta(\eta)$ as Nr uplifts in the heat area.

Figure 12 exhibits the reaction of the concentration profile to variations in Sc. Here, critical observation reveals that higher values of Sc diminishes the boundary structure and with that occurrence, the lowering of $\phi(\eta)$ is established as demonstrated in this plot. There is a conformity with this trend and the physics of the model since large values of Sc imply that there is less mass diffusivity, the consequence of which deteriorates the concentration boundary layer film.

Finally, the velocity profiles versus η for different values of We is evaluated in Fig.13. A growth in We is found to impede the speed of the fluid because as the relaxation time increases there is a generation of the drag like force at the speed profile.

5. Concluding remark

An assessment of the Williamson fluid comprising of tiny particles on a two-dimensional expanding plate is the focus of this study. The problem is considered in the neighbourhood of stagnation-point with convective heat condition, activation energy, chemical reaction, and irregular movement and thermo-movement of the tiny particles. The main equations are numerically solved while the impact of the emerging physical terms is appropriately explained with the aid of graphs. More so, under some limiting scenarios, the current solution is adjudged valid when verified with existing data in the literature. We realised from the study that:

- An expanding heat boundary film exists with higher values of the magnetic field term, Eckert number, Biot number, radiation and thermophoresis parameters but there is a contraction in the thermal field with the Prandtl number and velocity ratio.
- There is a depreciation in the hydrodynamic boundary film and the speed of the fluid with the magnetic field and material parameters but the reaction changes when the velocity ratio term is raised.
- There is contraction in the solutal boundary layer field due to a raise in the magnitude of the chemical reaction term, Schmidt number, thereby leading to a downward trend in the concentration profile but activation energy reacts differently as it raises the concentration field.

Acknowledgements

The authors thank the management of Bowen University for enabling environment provided and their continuous support to carry out this research work.

Nomeclature

A – velocity ratio

AE – activation energy

B_0 – magnetic field strength

c – stretching rates

Cr – chemical reaction

E_a – activation energy ratio

Ec – Eckert number

h – Biot number

K – thermal conductivity

k_1 – mean absorption coefficient

M – magnetic term

N – fluid concentration

NT – Brownian motion

Nr – thermophoresis

N_∞, – far stream concentration

T – liquid temperature

T_f – surface temperature

T_∞ – far stream temperature

u,v – velocity modules

We – material term

Γ – thermal conduction

δ – radiation term

μ – dynamic viscosity

ρ – density

σ – relaxation time

ϑ – kinematic viscosity

References

[1] Qasim M., Khan I. and Shafie S. (2013): H*eat transfer in a micropolar fluid over a stretching sheet with newtonian heating*.– PLOS ONE vol.8, pp.1-6.

[2] Crane L.J. (1970): *Flow past a stretching plate*.– Communications Breves, vol.21, pp.645-647.

[3] Gupta P.S. and Gupta A.S. (1977): *Heat and mass transfer on a stretching sheet with suction or blowing*.– Canadian Journal of Chemical Engineering, vol.55, pp.744-746.

[4] Chakrabarti A. and Gupta A.S. (1979): *Hydromagnetic flow and heat transfer over a stretching sheet.*– Quarterly of Applied Mathematics, vol.37. pp.73-78.

[5] Grubka L.J. and Bobba K.M. (1985): *Heat transfer characteristics of a continuous, stretching surface with variable temperature*.– Journal of Heat Transfer, vol.107, pp.248-250.

[6] Elbashbeshy E.M.A. and Bazid M.A.A. (2004): *Heat transfer in a porous medium over a stretching surface with internal heat generation and suction or injection.*– Applied Mathematics and Computation, vol.158, pp.799-807.

[7] Kumar L. (2009): *Finite element analysis of combined heat and mass transfer in hydromagnetic micropolar flow along a stretching sheet*.– Comput. Mater. Sci., vol.46, pp.841-848.

[8] Fatunmbi E.O. and Adeniyan A. (2018): *Heat and mass transfer in MHD micropolar fluid flow over a stretching sheet with velocity and thermal slip conditions*.– Open Journal of Fluid Dynamics, vol.8, pp.195-215.

[9] Shah Z., Kumam P. and Deebani W. (2020): *Radiative MHD Casson nanofluid flow with activation energy and chemical reaction over past nonlinearly stretching surface through entropy generation*.– Scientific Reports, vol.10, pp.1-14.

[10] Fatunmbi E.O. and Okoya S.S. (2020): *Heat transfer in boundary layer magneto-micropolar fluids with temperature-dependent material properties over a stretching sheet.*– Advances in Materials Science and Engineering, vol.20, pp.1-11.

[11] Williamson R.V. (2019): *The flow of pseudoplastic materials*.– Industrial and Engineering Chemistry, vol.21, pp.1108-1111.

[12] Khan N.A. and Khan. H.A (2014): *Boundary layer flows of non-Newtonian Williamson fluid*.– Nonlinear Engineering, vol.3, No.2, pp.107-115.

[13] Hayat T., Shafiq A. and Alsaedi A. (2016): *Hydromagnetic boundary layer flow of Williamson fluid in the presence of thermal radiation and Ohmic dissipation*.– Alexandria Eng. J., vol.43, pp.387-394

[14] Megahed A.M. (2019): *Williamson fluid flow due to a nonlinearly stretching sheet with viscous dissipation and thermal radiation*.– Journal of the Egyptian Mathematical Society, vol.27, pp.124322.

[15] Batool K. and Ashraf M. (2013): *Stagnation point flow and heat transfer of a magneto-micropolar fluid towards a shrinking sheet with mass transfer and chemical reaction*.– Journal of Mechanics, vol.29, pp.411-422.

[16] Ishak A., Jafar K., Nazar R. and Pop I. (2009): *MHD Stagnation point flow towards a stretching sheet*.– Physica A, vol.388, pp.3337-3383.

[17] Chiam T.C. (1994): *Stagnation-point flow towards a stretching plate*.– Journal of Physical Society of Japan, vol.63, pp.2443-2444.

[18] Mohapatra T.R. and Gupta A.S. (2002): *Heat transfer in stagnation point flow towards a stretching sheet*.– Heat and Mass Transfer, vol.38, pp.517-521.

[19] Monica M., Sucharitha J. and Kumar Ch.K. (2016): *Stagnation point flow of a Williamson fluid over a nonlinearly stretching sheet with thermal radiation*.– American Chemical Science Journal, vol.13, pp.1-8.

[20] Agbaje T.M, Mondal S., Makukula C.G., Motsa S.S. and Sibanda P. (2017): *A new numerical approach to MHD stagnation point flow and heat transfer*.– Ain Shams Engineering Journal, vol.9, pp.233-243.

[21] Choi S.U.S. and Eastman J.A. (1995): *Enhancing thermal conductivity of fluids with nanoparticles*.– No. ANL/MSD/CP-84938; CONF-951135-29. Argonne National Lab., IL (United States)

[22] Alsaedi A., Hayat T., Qayyum S. and Yaqoob R. (2020): *Eyring-Powell nanofluid flow with nonlinear mixed convection: entropy generation minimization*.– Computer Methods and Programs in Biomedicine, vol.186, pp.1-12.

[23] Al-Khaled K., Khan S.U. and Khan I. (2020): *Chemically reactive bioconvection flow of tangent hyperbolic nanoliquid with gyrotactic microorganisms and nonlinear thermal radiation*.– Heliyon, vol.6, pp.1-7.

[24] Mabood F. and Das K. (2016). *Melting heat transfer on hydromagnetic flow of a nanofluid over a stretching sheet with radiation and second order slip*.– Eur. Phys. J. Plus, vol.131, pp.1-11.

[25] Dzulkifli N.F., Bachok N., Yacob N.A., Arifin N. and Rosali H. (2018): *Unsteady Stagnation-Point flow and heat transfer over a permeable exponential stretching/shrinking sheet in nanofluid with slip velocity effect: A stability analysis*.– Appl. Sci., vol.8, pp.2172.

[26] Noor N.F.M., Haq R.U., Nadeem S. and Hashim I. (2015): *Mixed convection stagnation flow of a micropolar nanofluid along a vertically stretching surface with slip effects*.– Meccanica, vol.15, pp.1-16.

[27] Mukhopadhyay S., De P.R., Bhattacharyya K. and Layek G.C. (2012*): Forced convective flow and heat transfer over a porous plate in a Darcy-Forchheimer porous medium in presence of radiation*.– Meccanica, vol.47, pp.153-161.

[28] Ullah I., Shafie S. and Khan I. (2016): *Effects of slip condition and Newtonian heating on MHD flow of Casson fluid over a nonlinearly stretching sheet saturated in a porous medium*.– Journal of King Saud University-Science, vol.32, pp.675-782.

[29] Fatunmbi E.O., Ogunseye H.A. and Sibanda P. (2020): *Magnetohydrodynamic micropolar fluid flow in a porous medium with multiple slip conditions*.– International Communications in Heat and Mass Transfer, vol.115, pp.1-10.

[30] Patel H.R. (2019): *Effects of cross diffusion and heat generation on mixed convective MHD flow of Casson fluid through porous medium with non-linear thermal radiation*.– Heliyon, vol.5, pp.1-26.

[31] Mabood F. and Das K. (2016): *Melting heat transfer on hydromagnetic flow of a nanofluid over a stretching sheet with radiation and second-order slip*.– Eur. Phys. J. Plus, vol. 131, pp.477-485.

[32] Xu L and Lee E.W.M. (2013): *Variational iteration method for the magnetohydrodynamic flow over a nonlinear stretching sheet*.– Abst. Appl. Anal. vol.34, p.5.

Received: December 27, 2022
Revised: June 30, 2023